ACS OMEGA

http://pubs.acs.org/journal/acsodf

Article

Optimization of Surfactant- and Cosurfactant-Aided Pine Oil Nanoemulsions by Isothermal Low-Energy Methods for Anticholinesterase Activity

Mayank Handa, Rewati Raman Ujjwal, Nupur Vasdev, S. J. S. Flora, and Rahul Shukla*

Cite This: *ACS Omega* 2021, 6, 559−568

Read Online

ACCESS | Metrics & More | Article Recommendations | Supporting Information

ABSTRACT: Highly stable pine oil-loaded nanoemulsions were evaluated for nutraceutical and storage stability applications. Pine oil-loaded nanoemulsion preparation was done with pine oil as the oily phase and additionally with different ratios of the non-ionic surfactant (Tween 80) and cosurfactant (ethanol) in an aqueous solution using the isothermal low-energy or spontaneous emulsification method. A transparent and stable nanoemulsion was obtained with a combination of pine oil (5 wt %), surfactant mixture (35 wt %), and water quantity sufficient (qs) by the isothermal low-energy method. The mean droplet size and ζ-potential of the fabricated nanoemulsion were ≈14 nm and −3.4 mV, respectively. The size of the transparent nanoemulsion increased to ∼45 nm and showed turbidity at 60 °C. Microrheological investigation highlighted the gel−sol−gel conversion in the presence of applied angular frequency at 25 °C. The loss modulus shifted to lower frequency at 60 °C in comparison to other temperatures. The anticholinesterase (AChE) inhibition activity of the pine oil-loaded nanoemulsion suggested a possible therapeutic value, and at 0.10% concentration of the nanoemulsion, the AChE inhibition activity was ≈95.72 ± 5.59%. These studies have important implications in fabrication and optimization of a nanoemulsion as a delivery system for combating reminiscence in Alzheimer's disease and application in the nutraceutical-based industry. This isothermal low-energy method offers an advantage of preparing an edible oil delivery system using simple and rapid operational parameters.

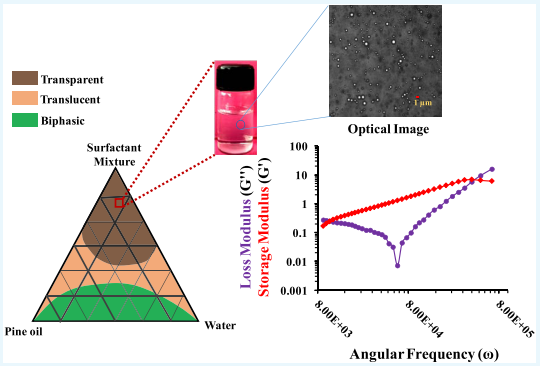

INTRODUCTION

Nanoemulsions are colloidal metastable dispersions of immiscible liquid phases of ∼200 nm, in which one phase is dispersed in the other continuous phase.[1−3] Natural-oil-based nanoemulsions have been explored for various applications such as neuroprotective,[4] chemotherapeutic,[5,6] antibacterial,[7] and aromatherapy. Lucian and co-workers reported the protective effect of pine oil against the induced oxidative stress due to amyloid β_{1-42}.[8] Similarly, Unstun and co-workers have studied the significance of the oil extract of *Pinus* in the anticholinesterase (AChE) activity in *in vitro* and *in vivo* models of Alzheimer's disease.[9]

When natural oils are administered in bodily fluids, nanoemulsions of natural oil show instability at lower or higher pH, thermal degradation, and high first-pass metabolism.[10] One of the major problems in the application of nanoemulsions is their method of preparation; a suitable method can be developed for minimization of droplet sizes and, therefore, natural-oil-based nanoemulsions are prepared by the isothermal low-energy method.[11] Preparation methods for nanoemulsions are categorized mainly as low-energy and high-energy techniques.[12]

A high-energy technique breaks emulsions into small droplets with the use of shear, cavitational, and turbulent forces. High-speed homogenization and sonication methods are the examples of high-energy techniques based on the same principle.[13] However, the low-energy technique involves energy barrier phenomena, which decrease the interfacial energy barriers between oil and the aqueous phase based upon solubility, and surface active agents.[14] The emulsion inversion point, spontaneous emulsification, phase inversion composition, and phase inversion temperature (PIT) methods are the examples of low-energy techniques. Low-energy techniques have advantages of being cost-effective, formation of small size droplets, and high surface mixture ratios.[15−17]

Based upon the droplet size, oil volume fraction, and emulsifier concentration, nanoemulsions show various rheological behaviors at the molecular level.[18,19] In dynamic light

Received: October 15, 2020
Accepted: November 24, 2020
Published: December 30, 2020

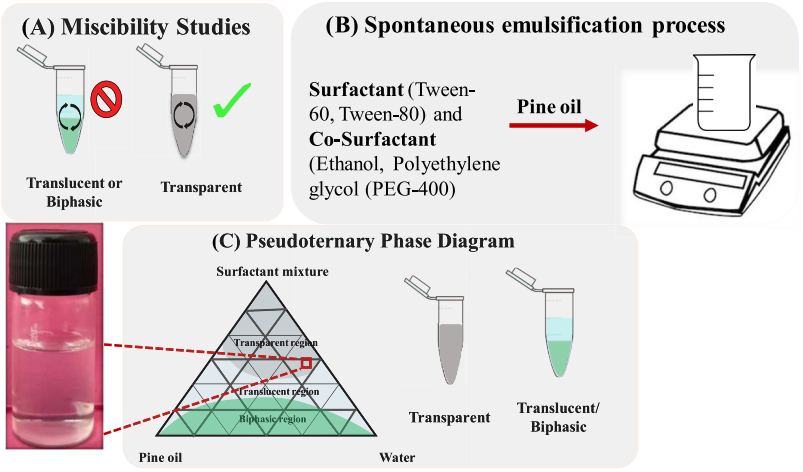

Figure 1. Schematic representation of (A) miscibility studies, (B) spontaneous emulsification process, and (C) pseudoternary phase diagram for the nanoemulsion preparation process.

scattering (DLS)-based microrheology or diffusive wave spectroscopy (DWS), temporary tracer particle fluctuations are measured as a function of diffusion and rearrangement of particles. Microrheology-based studies are being explored for studying the micellar gelation of casein in manufacturing of cheese and yogurt, where increase in loss modulus was observed with conversion from a sol to a gel state.[20,28] Similarly, the non-ionic surfactant Tween 40 and light mineral oil were used as a stabilizer for oil-in-water nanoemulsions with negative charge on the oil droplets and surrounded by charged counter ions.[21−23] The DLS-based microrheological study was dependent on the measurement of size and movement of tracer/probe particles with respect to medium in which they were incorporated. When the size of tracer particles was larger than that of the sample particles, then macroscopic parameters were evaluated, while when the tracer particle size was small, then commonly explored rheological properties were evaluated.

In this study, evaluation of colloidal carriers formulated using the low-energy isothermal method, i.e., the spontaneous emulsification method, was performed for fabrication of the pine oil clear nanoemulsion with a futuristic approach for therapeutic application in Alzheimer's disease. In this method, we have utilized the simple titrimetric method, which involves an oily phase with the surfactant mixture and addition of the aqueous phase followed by continuous mixing at room temperature.

To the best of author's knowledge, fabrication of a pine oil nanoemulsion involving spontaneous emulsification is not reported till date. This is a spontaneous approach in which the nanoemulsion is fabricated at room temperature without involving the expensive high-energy method. The prepared nanoemulsion was oil-in-water (O/W) in nature. Based on this hypothesis, this methodology can be explored in industrial applications involving both pharmaceutical and food-based industries for translational application.

RESULTS AND DISCUSSION

Miscibility studies are considered as an important parameter for the formulation of nanoemulsions by the spontaneous emulsification method (Figure 1A). Three types of solutions were observed. The translucent or biphasic nature of solution suggests least compatibility because of a high interfacial energy barrier since the pine oil was not miscible with Tween 20 and 40 due to short fatty acid chains, i.e., lauric acid and palmitic acid associated with the polyoxyethylene moiety of Tween.[31,32] These small fatty acids as parts of Tween were unable to reduce the interfacial energy barrier with pine oil. The transparent solution was formed due to lower interfacial energy barriers between the oil and surfactant. In the case of Tween 60 and 80, long-chain fatty acid groups of stearic acid and oleic acid are available that decrease the interfacial tension between the pine oil and surfactant.

Similar studies were also performed with poly(ethylene glycol) (PEG) series. Pine oil was not miscible with PEG 200 and 300 due to less number of hydroxyl (−OH) groups present on the PEG moiety, whereas PEG 400 was found to be miscible with pine oil due to enough OH groups[33] (Supporting Information SI, Table S1). The presence of hydroxyl groups enables efficient binding of oil components with glycol moieties due to intermolecular hydrogen bonding. But in the case of PEG 600, miscibility of pine oil was not observed due to intramolecular hydrogen bonding of PEG 600, which decreases the binding of glycol groups with oil, and translucent nature was observed.[34,35] Pine oil was miscible in ethanol and immiscible in water. Mono-alcoholic or poly-alcoholic moieties are preferred as cosurfactants because of their strong hydrogen bonding with water, ultimately decreasing the interaction of water with the oily phase. The surfactant and cosurfactant play an important role in the final selection of nanoemulsion formulations, since the surfactant decreases the interfacial tension and the cosurfactant holds the excess of aqueous phase by hydrogen bonding.[21,36] Based upon miscibility data, Tween 60 & 80, and ethanol and PEG 400 were selected as the surfactant and cosurfactant, respectively (SI, Table S1).

The pseudoternary phase diagram facilitates understanding of the spontaneous emulsification method for further studies (Figure 1). The pseudoternary phase diagram showed transparent, translucent, and biphasic regions and are marked with different colors (Figure 1C). Pseudoternary phase diagrams were plotted against pine oil, the surfactant mixture comprising Tween 60 along with ethanol and PEG 400, and the aqueous phase. Nanoemulsions obtained with the surfactant mixture of Tween 60 and ethanol as well as Tween 60 and PEG 400 were biphasic in nature. A higher amount of surfactant was required for obtaining a transparent

https://dx.doi.org/10.1021/acsomega.0c05033
ACS Omega 2021, 6, 559−568

nanoemulsion region, which was not acceptable from a regulatory point of view because of the toxic behavior at higher amounts.[37] The possible reason for obtaining less number of transparent nanoemulsion regions with this surfactant mixture might be the incompetency of Tween 60 to decrease the interfacial energy barrier of the system with pine oil. This was concluded from the trials with a variation in the concentration of Tween 60. Even with an increase in the ratio of Tween 60 to the cosurfactant from 1:1 to 2:1, no effect on the transparent nanoemulsion region was observed. This was not the case with Tween 80 when used as a surfactant. When Tween 80 was used with PEG 400 as a surfactant mixture, then not much clear nanoemulsion regions were obtained. By varying the ratio of Tween 80 and PEG 400 from 1:1 to 1:2 and 2:1, no increment in the clear nanoemulsion region was observed (SI, Tables S4−S6 and Figures S1−S3). The possible reason for this observation was that PEG 400 was not able to hold the water molecules in itself or the hydrogen bonding of the glycol moiety of PEG 400 and the hydroxyl moiety of water was weak. Broadly speaking, water molecule cohesive forces are stronger than water−glycol adhesive forces.[38] Further, as the pine oil concentration was increased from 5 to 10 wt %, there was a drastic decrease in the clear nanoemulsion region. Clear nanoemulsion regions in the presence of the Tween 80 and PEG 400 system were observed at higher surfactant concentrations, which is a limitation for pharmaceutical application. Maximum transparent nanoemulsions were observed in the surfactant mixture of Tween 80 and ethanol (in 1:1, 1:2, and 2:1) (SI, Tables S7−S9 and Figures S4−S6). This could be due to minimization of interfacial energy barriers by the surfactant mixture of Tween 80 and ethanol, which was not similarly observed with other surfactant mixtures (Tween 80 and PEG 400, Tween 60 and ethanol, and Tween 60 and PEG 400). Observation of translucent, biphasic, or heterogeneous nanoemulsion regions could be due to Ostwald ripening or coalescence of pine oil in the respective surfactant mixture and pine oil and water ratios.[26] This can be correlated with the phase behavior of pine oil also at certain compositions when mixed with the surfactant mixture−water−oil system. The concentration of pine oil had a major effect on the nanoemulsion and emulsion formation when the spontaneous emulsification process was employed. Pine oil itself was not sufficient to formulate into a stable nanoemulsion form, and the emulsions fabricated by this were highly unstable and mainly exist in a heterogeneous form.[39] For formulation of a transparent nanoemulsion, a proper mixture of surfactants was required in an appropriate ratio. When the concentration of pine oil was varied from 20 to 35 wt %, the nanoemulsion system tends to formulate an unstable and heterogeneous type of system.

The surfactant effect on the clear nanoemulsion region was also evaluated using varying amounts of surfactant and mixtures with various pine oil concentrations. With an increase in surfactant concentration, there was high possibility of obtaining an optically clear nanoemulsion because of minimizing the droplet.[40] An optically opaque nanoemulsion might be due to a large droplet size occurring because of the phase behavior. When pine oil was kept at 5 wt % total nanoemulsion with 35 wt % surfactant mixture, then a clear nanoemulsion was obtained, while when the oil was kept at 10 wt % and similarly 35 wt % surfactant mixture was used, then opacity was observed in the formulated nanoemulsion (SI, Tables S6−S9 and Figures S4−S6). This might be due to the effect of surfactant concentration in the system, which ultimately fails to reduce the interfacial tension among the different phases of the pine oil−surfactant−water admixture. When the concentration of Tween 80 was varied using different ratios of the surfactant mixture, not much difference was observed in the nanoemulsion region. This might be due to the phase behavior of the ternary system that was used.

The surfactant type depends on its nature, that is, whether it is an ionic or a non-ionic surfactant, and also on the hydrophilic−lipophilic balance (HLB) of the surfactant. In the present investigation, selection of non-ionic surfactant was favored because of its broad regulatory acceptance in food as well as the pharmaceutical industry. The Tween or chemically polysorbate series is widely accepted by the United States Food and Drug Administration (US FDA) and generally regarded as safe (GRAS). Difference in Tween 20, 40, 60, and 80 is due to the chain length of the moiety. As the Tween numeric increases, i.e., from 20 to 80, indicate the chain length increases due to the attachment of different fatty acid moieties to it. Increase in chain length provides more steric hindrance and enhanced phase behavior with a decrease in overall interfacial energy of the system. Similarly, in the investigation, when Tween 60 was incorporated in the nanoemulsion system, not much fruitful optically clear nanoemulsion regions were observed, but the same was not observed with the Tween 80 system.[49] Tween 80-formulated nanoemulsion systems provide a highly stable and optically clear nanoemulsion (SI, Tables S4−S9). This might be due to the attachment of the fatty acid moiety, i.e., oleic acid chains, with the sorbitan moiety in Tween 80, which provides more steric hindrance in comparison to that from the palmitic acid moiety attached to Tween 60.[41]

Similarly, various cosurfactants were also investigated for nanoemulsion formulation. In the present investigation, PEG 400 and ethanol were screened out using miscibility studies. But not much clear regions were found with cosurfactant PEG 400, whereas ethanol showed a large number of clear nanoemulsions. This might be due to higher hydrogen binding of ethanol than PEG 400 with water. For example, 5 wt % pine oil, 35 wt % surfactant mixture (Tween 80 and PEG 400, 1:1), and rest 60 wt % water were observed to form a biphasic nanoemulsion (SI, Table S4). Similarly, when keeping all of the stated concentrations the same, just by changing the cosurfactant from PEG 400 to ethanol, there was a drastic paradigm shift in optical observation of the nanoemulsion. The nanoemulsion was found to be optically clear and stable (SI, Table S7).

From all of the above observations, it was inferred that the pine oil concentration must be kept below 35% of total weight. As the pine oil concentration increases manifold times, observance of optical clarity decreases. Possible reasons for the decrease in optical clearance of formulated nanoemulsions can be the increase in interfacial tension at the boundary of oil and water and genesis of Ostwald ripening, finally affecting the optical observation of nanoemulsions.[42,43]

As per the scale bar in Figure 2, the droplet was <500 nm. The count of the droplet was found to be less, which might be due to the low detection limit of the optical microscope.[50] In microscopy, emulsion droplets were measured with both dark and bright fields for better understanding of the droplet shape. The shape of the droplet in Figure 2 was found to be spherical. Further, at room temperature, small-sized droplets were

https://dx.doi.org/10.1021/acsomega.0c05033
ACS Omega 2021, 6, 559−568

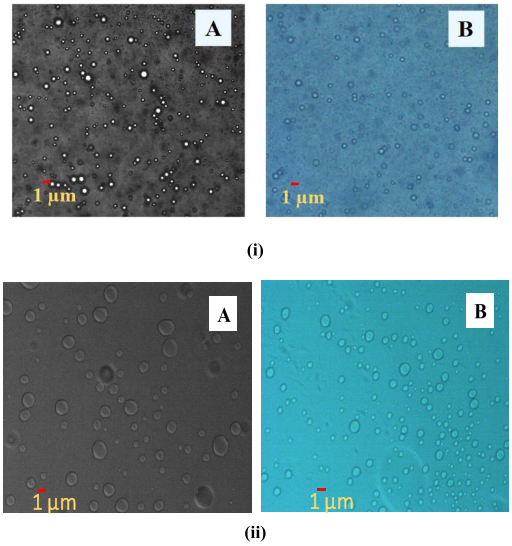

Figure 2. Optical microscopy images of the nanoemulsion droplets at (i) room temperature and (ii) 60 °C under dark field (A) and bright field (B).

observed in Figure 2-i, and similarly when observed at 60°C, larger-sized droplets were observed in Figure 2-ii.

Thermal Analysis Using DLS and Ultraviolet (UV) Techniques. Formulated nanoemulsions were subjected to thermal treatment for industrial applications. Therefore, the present investigation was also focused on thermal behavior studies using simultaneously three different techniques. A clear nanoemulsion forms small size droplets, i.e., in the nanoscale range. For observing the size of droplets in the clear nanoemulsion region, the dynamic light scattering (DLS) technique was used, which measures the Brownian motion of nanoemulsion droplets. For thermal analysis of the nanoemulsion, the DLS technique was employed in which temperature was increased from 20 to 70 °C and the size of nanoemulsion droplets was measured using the principle of DLS. Another technique used for analyzing the thermal stability of the selected nanoemulsion was UV−vis thermoanalysis. In this, a ramp at a rate of 5 °C/min was applied from 20 to 70 °C, scanning was done from 700 to 600 nm, and absorbance was analyzed, which was then converted into turbidity using eq 1. The last method employed for studying thermal analysis was graphical representation, in which visual or real-time imaging was done after every 10 °C with a starting temperature of 20 °C and end point at 70 °C.[44] We investigated the thermal stability of the formulated clear F1 nanoemulsion (comprising 5 wt % pine oil, 35 wt % surfactant mixture (equivalent ratio of Tween 80 and ethanol, 1:1), and 60 wt % water) (SI, Table S7 and Figure S4) by the above-stated method. During the initial phase of the study, the sample of the formulated nanoemulsion was optically clear at 20 °C and the droplet size measured by the DLS method was observed to be ≈12 nm. But as the temperature increased up to 50 °C, no much change in the droplet size was observed. The sizes of the F1 nanoemulsion at 30, 40, and 50 °C were ≈12, 12, and 15 nm, respectively (Figure 3). The postulation of these observations might be the stability of pine oil in the phase preparation of Tween 80 and ethanol, where no coalescence of particles was observed. But at 60 °C, the droplet size was observed to be ≈44 nm. The authors postulate that this might be due to coalescence of oil droplets and can be

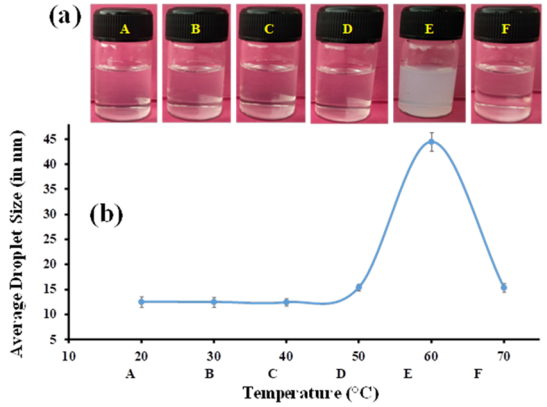

Figure 3. (a) Images and (b) size distribution of the transparent nanoemulsion at 20, 30, 40, 50, 60, and 70 °C.

attributed to the fact that as the temperature rises the phase change might also take place and pine oil droplets tend to supersede interfacial barriers and move toward cohesiveness. This can also be related to the phase transition of the nanoemulsion phase where it surpassed the phase inversion temperature (PIT) and resulted in conversion of the oil-in-water system to a water-in-oil system (Figure 4). But as the increment in temperature took place from 60 to 70 °C, there was a dip in the droplet size of the nanoemulsion and was observed to be ≈15 nm. This might be due to formation of microemulsion in and around PIT, which states that formulation of a nanoemulsion takes place at lower temperature.[26] The conductivity study showed that the conductivity was a function of temperature. With the increase of temperature from 20 to 70 °C, the conductivity was also increased from 25.2 to 42.8 (μS/cm) (SI Figure S8). But from 60 to 70 °C, there was a slight decrement of conductivity that might be attributed to conversion of the oil-in-water nanoemulsion to the water-in-oil nanoemulsion. These observations are also in line with above-stated DLS-based and UV-based turbidity studies.

Scanning of the sample was done at two λ (wavelength) values, i.e., 600 and 660 nm. Starting initially from 20 °C, absorbance was measured and converted into turbidity using eq 1 as mentioned in materials and methods. Absorbance, turbidity, or both observed at temperature 50 °C were nearly equivalent to the turbidity observed at 20 °C temperature.

A steep increase in absorbance or turbidity was observed at 60 °C due to conversion of the oil-in-water-based colloidal system to the water-in-oil colloidal system; broadly speaking, 60 °C was observed to be the phase inversion temperature (PIT) or more preferably aggregation of oil droplets took place. After an increase in temperature to 70 °C, there was a steep decrease in absorbance or turbidity (Figure 5). Postulation of this observation might be attributed with DLS analysis, stating that with formation of clear microemulsion at higher temperature.[26]

DWS-Based Microrheological Investigation. Microrheological experiments were performed for the selected nanoemulsion with the optimized combination of 5 wt % pine oil and 35 wt % surfactant using a single-probe particle tracking system. The dynamic modulus (storage and loss moduli) of the nanoemulsion was calculated at different angular frequencies. A sharp "V shape" dip at 6.06×10^4 rad/s was observed in the loss modulus profile, which could be due

https://dx.doi.org/10.1021/acsomega.0c05033
ACS Omega 2021, 6, 559−568

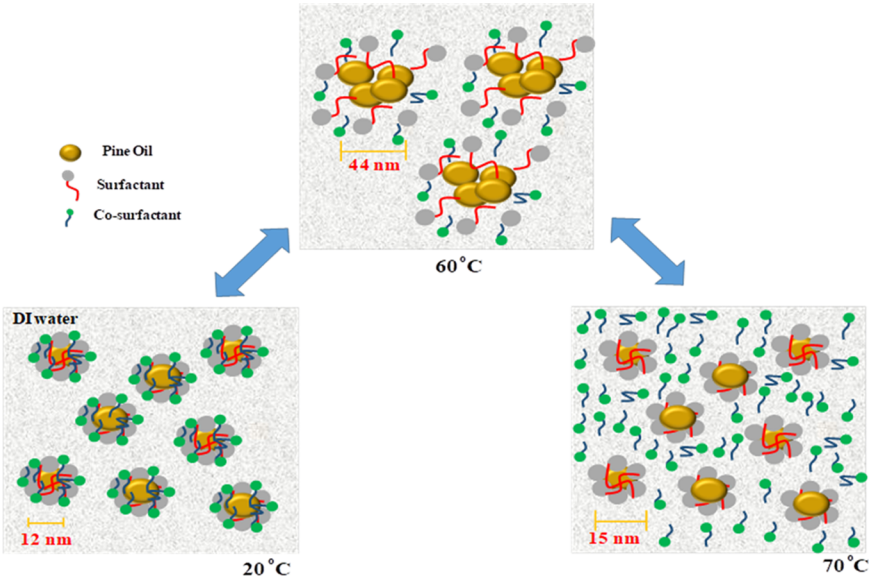

Figure 4. Schematic illustration of nanoemulsion droplets at different temperatures.

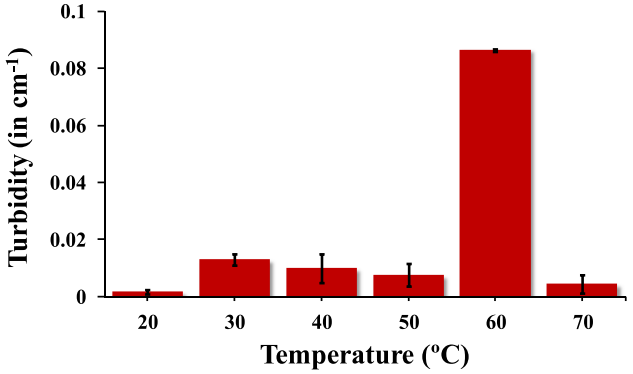

Figure 5. Turbidity study of the nanoemulsion at 600 nm from 20 to 70 °C.

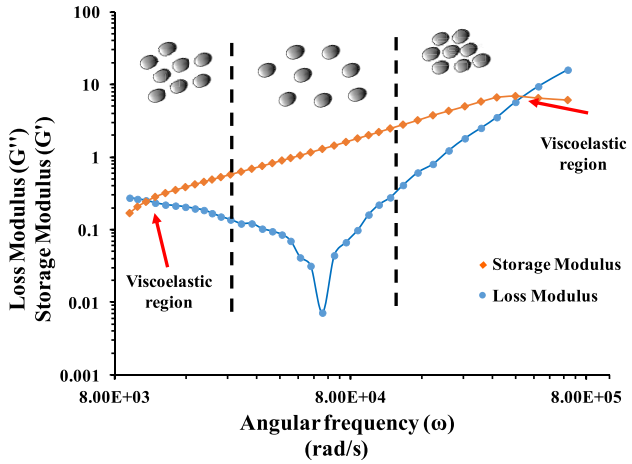

Figure 6. Microrheological analysis: frequency-sweep measurements as a function of loss (G'') and storage (G') moduli for the transparent nanoemulsion using the DWS passive technique at 25 °C.

to coupling of tracer particles with droplets of the nanoemulsion and pragmatic vibrations, which made the colloidal molecules discrete[20,51] (Figure 6). With an increase in the angular frequency, the loss modulus increases due to transformation of the nanoemulsion from sol to gel (Figure 6).

These explanations clearly described the effect of applied conditions on the phase performance of the colloidal systems. Before the dip state, the molecular separation phase existed where an increment in vibrational frequency caused separation of molecules because of the decrease in cohesive forces among the colloidal molecules (Figure 6). But there was a dip point where tracer particles might have interacted with colloidal particles and overcome the decrease in cohesive forces. After the dip, as the vibration frequency increment took place, the molecules started coming closer to each other, which directly paved the way for increment in molecular cohesive forces, and the sol-to-gel conversion took place.[20,45]

This study was extended for assessing the temperature-dependent modulus behavior, where we observed that the loss modulus was shifted at 60 °C in comparison to room temperature. A sharp decrease in loss moduli at this temperature might be due to the high rate of Ostwald ripening (Figure 7). The temperature study was also in support of the thermal analysis of the nanoemulsion (turbidity and droplet size studies). Similarly, in complex viscosity analysis (Figure 8), high values of complex viscosity parameters were observed at 60 °C.

This might be due to the high rate of Ostwald ripening particularly at 60 °C. But a similar pattern was not observed at 65 or 70 °C because of the phase conversion temperature at this point only. As the angular frequency was increased, the complex viscosity also decreased. This might be due to separation of closely associated nanoemulsion droplets, which caused a linear decrease in complex viscosity. Further, complex viscosity was almost similar at other temperatures (40, 50, 55, 65, and 70 °C) when compared to 60 °C. From above studies, it was inferred that 60 °C is the phase inversion temperature where nanoemulsions are converted to microemulsions.

Storage Stability Studies. For the very commercial or pharmaceutical application of any product, it becomes necessary to have a proper storage shelf life, where a product has to be stable for a definite period of time, with no alteration in its particle size, polydispersity index, and ζ-potential. Therefore, we determined the storage stability at three

https://dx.doi.org/10.1021/acsomega.0c05033
ACS Omega 2021, 6, 559−568

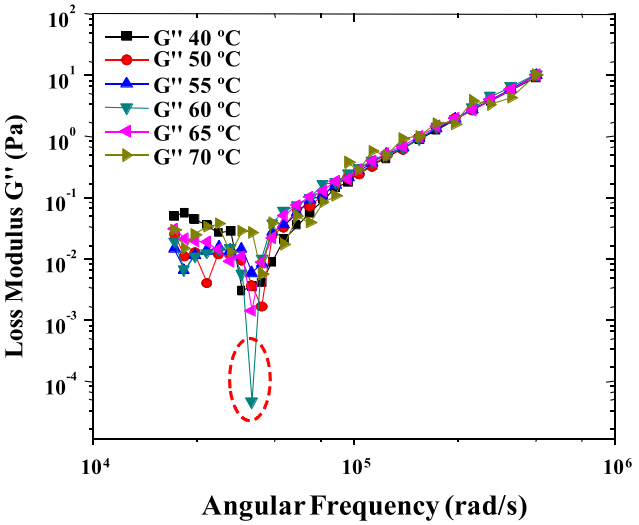

Figure 7. Effect of temperature on frequency-sweep measurements as a function of loss modulus (G'') for the transparent nanoemulsion.

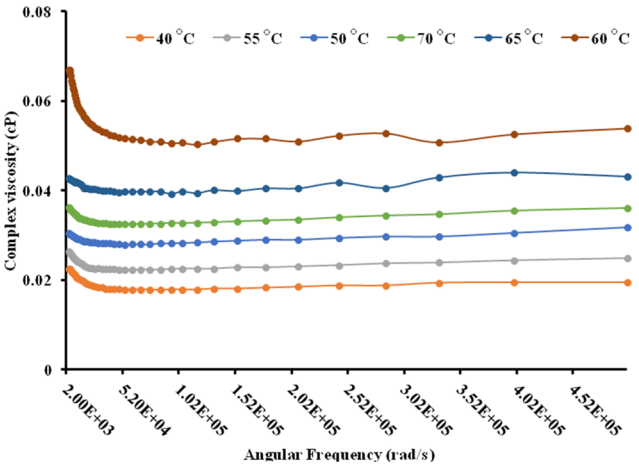

Figure 8. Effect of temperature on complex viscosity measurements of the transparent nanoemulsion.

temperature regimes, i.e., 4, 25, and 45 °C.[46−48] Selection of 4 °C temperature for a long term was done to confirm, at lower temperature, any effect on the droplet size with respect to any coalescence of oil droplets or increase of the interfacial energy barriers, which cumulatively impact enhancement in the particle size. Selection of 45 °C temperature was done to know whether storage at higher temperature causes separation of the phases and leads to coalescence of oil droplets. Examination of the droplet size in the representative sample, i.e., 5 wt % pine oil, 17.5 wt % Tween 80, 17.5 wt % ethanol, and 60 wt % water, was performed (Table 1).

As observed on the 0th day, the droplet size of the formulation was measured to be 13.93 nm with PDI of 0.083. When observed on the 7th day, droplet sizes observed at 4, 25, and 45 °C were 13.97, 14.13, and 14.09 nm, respectively. These observations might be due to the stability of oil droplets and properties of the surfactant mixture, which prevented coalescence of oil droplets at the respective temperature. Similarly, at the 14th day, the droplet sizes at above-mentioned conditions were 14.58, 13.56, and 12.97 nm, respectively. The stable droplet size of the pine oil-loaded nanoemulsion suggested that the phase behavior of the system was stable at the selected concentration. When observed on the 21st day, the droplet sizes at all three conditions were 14.24, 14.70, and 13.49 nm, respectively. Similarly, on the 28th day, the droplet sizes of the nanoemulsion at all conditions were 13.42, 15.21, and 14.71 nm, respectively (Figure 9A). Postulation for this observation was the concentration of the surfactant, which kept the system stable and prevented the coalescence of oil droplets at the different temperatures. Due to the presence of Tween 80 in the formulation, which is a non-ionic surfactant, the ζ-potential of the formulation was found to be near zero, i.e., −3.45 mV. No variation in ζ-potential data was observed when the nanoemulsion was stored at three different temperatures, 4, 25, and 45 °C (Figure 9B). This confirms that prepared nanoemulsions were stable at these temperatures and no coalescence or Ostwald ripening of oil droplets was observed.

Anticholinesterase (AChE) Activity of the Pine Oil-Loaded Nanoemulsion. The optimized pine oil-loaded nanoemulsion containing 5 wt % pine oil was subjected to AChE inhibition. The pine oil-loaded nanoemulsion was found to have good inhibitory properties with a dose-dependent relationship.

At a concentration of 0.00156% of the nanoemulsion, the AChE inhibition activity observed was 21.79 ± 2.06%, and the AChE inhibition activity further increased with an increase in the concentration of the nanoemulsion. At 0.0031% nanoemulsion concentration, AChE inhibition was 38.52 ± 2.16%. Similarly, at 0.006, 0.012, 0.025, 0.05, and 0.1% nanoemulsion concentrations, AChE inhibition values were 58.36 ± 1.59,

Table 1. Storage Stability Data of the Nanoemulsion at 4, 25, and 45 °C

No. of Days ⇩ Temperature ⇨	Particle size (in nm) ± S.D.			Zeta Potential (in mV)		
	4°C	25°C	45°C	4°C	25°C	45°C
0	-	13.93±0.27	-	-	-3.45	-
7	13.97±0.12	14.13±0.45	14.09±0.40	-4.56	-3.98	-4.02
14	14.58±0.17	13.56±0.51	12.97±0.78	-3.27	-4.69	-4.14
21	14.24±0.13	14.70±0.34	13.49±0.47	-3.66	-4.12	-3.47
28	13.42±0.33	15.21±0.28	14.71±0.42	-4.98	-3.23	-3.87

https://dx.doi.org/10.1021/acsomega.0c05033
ACS Omega 2021, 6, 559−568

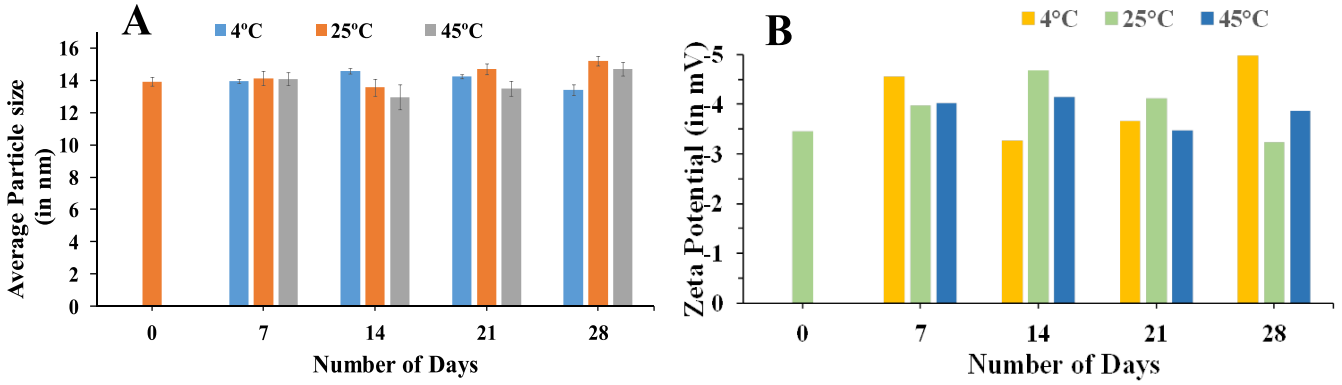

Figure 9. Storage stability analysis of the nanoemulsion at 4, 25, and 45 °C using (A) DLS and (B) ζ-potential with time.

75.09 ± 6.60, 85.60 ± 2.91, 92.21 ± 2.94, and 95.72 ± 5.59%, respectively (Figure 10).

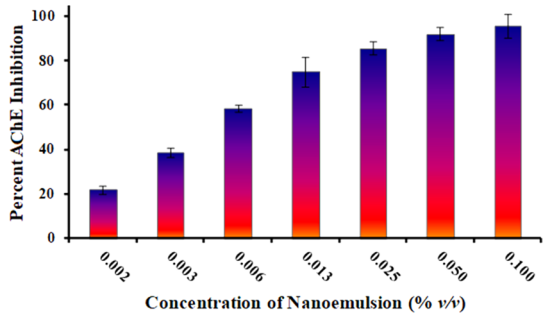

Figure 10. AChE inhibition activity of the pine oil-loaded nanoemulsion.

This dose-dependent relationship of the AChE inhibition activity of the pine oil-loaded nanoemulsion suggested a possible therapeutic value and in the near future can be considered as having a therapeutic potential for Alzheimer's management.

CONCLUSIONS

Thermodynamically stable pine oil-loaded nanoemulsions were prepared via the spontaneous emulsification process. Transparent pine oil nanoemulsions were prepared with Tween 80 and ethanol at a lower surfactant mixture concentration. The pine oil concentration played an important role in selection of a stable nanoemulsion. The thermal study of the nanoemulsion showed a phase inversion behavior at 60 °C and conversion of the oil-in-water system to the water-in-oil system. Microrheological studies showed a viscoelastic nature of the nanoemulsion, i.e., with an increase in angular frequency, there was an increase in aggregation or gelation. Storage data showed no much change in the droplet size of the selected nanoemulsion. The optimized pine oil nanoemulsion with an acceptable concentration of surfactants and cosurfactants may be utilized for therapeutic application in humans and its AChE inhibition potential. Advantages associated with the spontaneous emulsification method are simplification in implementation, low energy requirement, no requirement of expensive instrumentation, and low operational cost. Prepared nanoemulsions with the spontaneous emulsification method had a small droplet size in comparison to the nanoemulsion prepared with the high-energy method. The major disadvantage with the spontaneous emulsification method is the requirement of high surfactant concentration, which might be toxic. But this is not the case when the oil concentration is relatively low and thus it can be well applied in pharmaceutical, food, and beverage industries for various commercial applications.

MATERIALS AND METHODS

Pine oil was supplied by Sigma-Aldrich (CAS number: 8021-29-2, pine needle oil, natural, FG) and was composed of oils from different pine species such as *Pinus elliottii*, *Pinus palustris*, *Pinus taeda*, *Pinus serotina*, and *Pinus clausa*. Ethanol and methanol were purchased from Merck, India. Polysorbate or Tween (20, 40, 60, and 80) was purchased from SRL, India. Poly(ethylene glycol) (200, 300, 400, and 600) was purchased from Merck, India. Triple distilled water was obtained from Milli-Q millipore assembly by Merck.

Evaluation of Pine Oil Miscibility with Various Solvents. The miscibility study of pine oil was performed with different ratios of Tween series (20, 40, 60, and 80), poly(ethylene glycol) (PEG) series (200, 300, 400, and 600), ethanol, methanol, and water. In this study, pine oil was added to a 2 mL clear centrifuge tube followed by addition of an equivalent amount of above-mentioned components individually. After the addition of components, the centrifuge tube was kept on a vortex shaker for complete mixing of added components. Observation was made on the appearance of the solution to check whether it was transparent, translucent, or biphasic.[24,25] Miscibility of various mixtures was observed as transparent, translucent, and biphasic in nature.

Preparation of the Nanoemulsion and Pseudoternary Phase Diagram. The spontaneous emulsification method was employed for several batches of nanoemulsions. In this method, titration was performed with water and pine oil with varying the surfactant mixture. The final solution was mixed using a vortex shaker. Based upon visibility, three types of emulsions (transparent, translucent, and biphasic) were observed. Pseudoternary phase diagrams were plotted on the basis of the observation. The method employed pine oil (10% v/v), surfactant mixture (40% v/v containing Tween 80 and ethanol in equivalent 1:1 ratio), and water (50% v/v) with total cumulative value of all components not more than 100% v/v (oil + surfactant mixture + water).[26,27]

Evaluation of Particle Size Analysis. The particle size of the emulsion was analyzed using Zetasizer Malvern Nano ZS, Malvern Instruments Ltd., Worcestershire, U.K. Principle for the working of this instrument which determines the intensity of particle size from a laser beam at wavelength 633 nm with

https://dx.doi.org/10.1021/acsomega.0c05033
ACS Omega 2021, 6, 559−568

scattering angle of 173°. For each measurement, there exists an individual run of 13, and to avoid multiple scattering, proper dilution with water was made before measurements. Samples prepared were filtered by passing through a 0.45 μm syringe filter and diluting to a ratio of 1:100 (v/v) at 25 °C with triple distilled water, done in triplicate.

Observation of Emulsion Droplets by Optical Microscopy. An optical microscope (Leica-DM4AP model), Leica, Mumbai, India, was used to observe emulsion droplets diluted with triple distilled water in a 1:100 ratio. Images of droplets were captured at 20× magnification.

Evaluation of DWS-Based Microrheological Investigation. DWS spectroscopy of the emulsion was performed using Zetasizer Malvern Nano ZS, Malvern Instruments Ltd., Worcestershire, U.K. A carboxylated form of melamine particles (S2156) with a predetermined particle size of 615 nm provided by Malvern, U.K., was used as tracer particles. The very first step is to determine the ζ-potential of tracer particles by preparing a dilution of tracer particles in triple distilled water. The second step was to determine the compatibility of tracer particles with the fabricated nanoemulsion using the ζ-potential technique with a difference of ±5 mV between the tracer and the nanoemulsion sample. The third step was to determine the microrheology of the sample by incorporating tracer particles in the sample and measuring at various angular frequencies.[28]

Evaluation of Thermal Stability of the Nanoemulsion Using DLS and UV Techniques. Thermal stability of the nanoemulsion was determined using the DLS technique in which the temperature was increased from 20 to 70 °C and the sample particle size was determined with every 10 °C increment.[26] Similarly, critical microrheological investigation was also done by comparing the storage modulus, loss modulus, and complex viscosity parameters.

UV−vis spectroscopy analysis was used for thermal evaluation and was carried out on a Carry 100 series instrument, Agilent. A ramp from 20 to 70 °C was applied with an increment of 10 °C/min with measuring absorbance at wavelengths 600−660 nm, and water was used as a blank.[26] Concentrated samples were kept in the sampling port in a quartz cuvette. Absorbance was converted into turbidity (in cm^{-1}) using the formula

$$\text{turbidity} = 2.303 \times \frac{\text{absorbance}}{\text{path length (in cm)}} \quad (1)$$

Evaluation of Storage Stability Studies. The storage stability study was performed at three different conditions. The prepared nanoemulsion was checked for stability for four weeks at 4, 25, and 45 °C. Aliquots of the sample were taken out at 0, 7th, 14th, and 28th days and analyzed for particle size, polydispersity index, and ζ-potential with the repetitive procedure as mentioned in the above section.[29]

Evaluation of *In Vitro* Anticholinesterase (AChE) Activity. The AChE inhibition activity was tested using the microplate assay. The blank group, control group, and different dilutions of the sample were pipetted in 96-well microtiter plates in triplicate. Acetylthiocholine iodide (ATCI) was hydrolyzed by acetylcholinesterase to thiocholine and acetate, and this thiocholine was reacted with dithiobisnitrobenzoic acid (DTNB) to produce yellow color. The yellow color observed by the spectrophotometer indicates the hydrolysis of substrates and formation of 5-thio-2-nitrobenzoate anions.[30] Therefore, a higher yellow color intensity indicates more hydrolysis of acetylthiocholine and low yellow color intensity indicates the inhibition of hydrolysis of acetylcholine by acetylcholinesterase. In the blank group, pH 8.0 phosphate buffer, methanol, and the reaction mixture (75 mM ATCI and 10 mM DTNB) were added, and in the control group, acetylcholinesterase was added for complete inhibition. The sample was added in different dilutions from lower concentration to higher concentration to check the inhibition of acetylcholinesterase.

Blank: 130 μL PBS + 10 μL PBS + 10 μL methanol + 142 μL reaction mixture.

Control: 130 μL PBS + 10 μL AChE + 10 μL methanol + 142 μL reaction mixture.

Sample: 130 μL PBS + 10 μL AChE + 10 μL dilutions of nanoemulsion + 142 μL reaction mixture.

Excluding the reaction mixture, everything was pipetted in 96-well microtiter plates and incubated for 10 min. After 10 min, the reaction mixture was added and then 96-well plates were visualized in a microplate reader at 412 nm.

■ ASSOCIATED CONTENT

Supporting Information

The Supporting Information is available free of charge at https://pubs.acs.org/doi/10.1021/acsomega.0c05033.

Miscibility studies; emulsion preparation; pseudoternary phase diagrams; *in vitro* anticholinesterase activity; and conductivity studies (PDF)

■ AUTHOR INFORMATION

Corresponding Author

Rahul Shukla − *Department of Pharmaceutics, National Institute of Pharmaceutical Education and Research (NIPER)-Raebareli, Lucknow 226002, India;* orcid.org/0000-0002-4864-0133; Email: rahulshuklapharm@gmail.com

Authors

Mayank Handa − *Department of Pharmaceutics, National Institute of Pharmaceutical Education and Research (NIPER)-Raebareli, Lucknow 226002, India;* orcid.org/0000-0001-9093-6432

Rewati Raman Ujjwal − *Department of Pharmacology and Toxicology, National Institute of Pharmaceutical Education and Research (NIPER)-Raebareli, Lucknow 226002, India;* orcid.org/0000-0001-6016-0872

Nupur Vasdev − *Department of Pharmaceutics, National Institute of Pharmaceutical Education and Research (NIPER)-Raebareli, Lucknow 226002, India*

S. J. S. Flora − *Department of Pharmacology and Toxicology, National Institute of Pharmaceutical Education and Research (NIPER)-Raebareli, Lucknow 226002, India;* orcid.org/0000-0002-5700-8236

Complete contact information is available at: https://pubs.acs.org/10.1021/acsomega.0c05033

Author Contributions

M.H., R.R.U., and Nupur performed and designed the experiments. S.J.S.F. provided critical review of the manuscript, and R.S., M.H., and R.R.U. co-wrote the paper. All authors commented on the manuscript.

https://dx.doi.org/10.1021/acsomega.0c05033
ACS Omega 2021, 6, 559−568

Notes

The authors declare no competing financial interest.

■ ACKNOWLEDGMENTS

The authors acknowledge the Department of Pharmaceuticals, Ministry of Chemical and Fertilizers, Government of India, for financial support. The NIPER-R communication number for this article is NIPER-R/Communication/116.

■ REFERENCES

(1) Kadiya, K.; Ghosh, S. Conversion of Viscous Oil-in-Water Nanoemulsions to Viscoelastic Gels upon Removal of Excess Ionic Emulsifier. *Langmuir* **2019**, *35*, 17061−17074.
(2) Ozturk, B.; Argin, S.; Ozilgen, M.; McClements, D. J. Nanoemulsion Delivery Systems for Oil-Soluble Vitamins: Influence of Carrier Oil Type on Lipid Digestion and Vitamin D3 Bioaccessibility. *Food Chem.* **2015**, *137*, 8−17.
(3) Gué, E.; Since, M.; Ropars, S.; Herbinet, R.; Le Pluart, L.; Malzert-Fréon, A. Evaluation of the Versatile Character of a Nanoemulsion Formulation. *Int. J. Pharm.* **2016**, *498*, 49−65.
(4) Park, S. H.; Ryu, S. N.; Bu, Y.; Kim, H.; Simon, J. E.; Kim, K. S. Antioxidant Components as Potential Neuroprotective Agents in Sesame (*Sesamum indicum* L.). *Food Rev. Int.* **2010**, *26*, 103−121.
(5) Scotece, M.; Conde, J.; Abella, V.; Lopez, V.; Pino, J.; Lago, F.; Smith, A. B.; Gómez-Reino, J. J.; Gualillo, O. New Drugs from Ancient Natural Foods. Oleocanthal, the Natural Occurring Spicy Compound of Olive Oil: A Brief History. *Drug Discovery Today* **2015**, *20*, 406−410.
(6) da Silva, S. L.; Figueiredo, P. M. S.; Yano, T. Chemotherapeutic Potential of the Volatile Oils from Zanthoxylum Rhoifolium Lam Leaves. *Eur. J. Pharmacol.* **2007**, *576*, 180−188.
(7) Moghimi, R.; Ghaderi, L.; Rafati, H.; Aliahmadi, A.; Mcclements, D. J. Superior Antibacterial Activity of Nanoemulsion of Thymus Daenensis Essential Oil against *E. coli*. *Food Chem.* **2016**, *71*, 69−76.
(8) Postu, P. A.; Sadiki, F. Z.; El Idrissi, M.; Cioanca, O.; Trifan, A.; Hancianu, M.; Hritcu, L. Pinus Halepensis Essential Oil Attenuates the Toxic Alzheimer's Amyloid Beta (1-42)-Induced Memory Impairment and Oxidative Stress in the Rat Hippocampus. *Biomed. Pharmacother.* **2019**, *112*, No. 108673.
(9) Lee, J. S.; Kim, H. G.; Lee, H. W.; Kim, W. Y.; Ahn, Y. C.; Son, C. G. Pine Needle Extract Prevents Hippocampal Memory Impairment in Acute Restraint Stress Mouse Model. *J. Ethnopharmacol.* **2017**, *207*, 226−236.
(10) Turek, C.; Stintzing, F. C. Stability of Essential Oils: A Review. *Compr. Rev. Food Sci. Food Saf.* **2013**, *12*, 40−53.
(11) Singh, Y.; Meher, J. G.; Raval, K.; Khan, F. A.; Chaurasia, M.; Jain, N. K.; Chourasia, M. K. Nanoemulsion: Concepts, Development and Applications in Drug Delivery. *J. Controlled Release* **2017**, *252*, 28−49.
(12) Sutradhar, K. B.; Amin, L. Nanoemulsions: Increasing Possibilities in Drug Delivery. *Eur. J. Nanomed.* **2013**, *5*, 97−110.
(13) Qian, C.; McClements, D. J. Formation of Nanoemulsions Stabilized by Model Food-Grade Emulsifiers Using High-Pressure Homogenization: Factors Affecting Particle Size. *Food Hydrocolloids* **2011**, *25*, 1000−1008.
(14) Kotta, S.; Khan, A. W.; Ansari, S. H.; Sharma, R. K.; Ali, J. Formulation of Nanoemulsion: A Comparison between Phase Inversion Composition Method and High-Pressure Homogenization Method. *Drug Delivery* **2015**, *22*, 455−466.
(15) Komaiko, J. S.; Mcclements, D. J. Formation of Food-Grade Nanoemulsions Using Low-Energy Preparation Methods: A Review of Available Methods. *Compr. Rev. Food Sci. Food Saf.* **2016**, *15*, 331−352.
(16) Forgiarini, A.; Esquena, J.; González, C.; Solans, C. Formation of Nano-Emulsions by Low-Energy Emulsification Methods at Constant Temperature. *Langmuir* **2001**, *17*, 2076−2083.
(17) Ragelle, H.; Crauste-Manciet, S.; Seguin, J.; Brossard, D.; Scherman, D.; Arnaud, P.; Chabot, G. G. Nanoemulsion Formulation of Fisetin Improves Bioavailability and Antitumour Activity in Mice. *Int. J. Pharm.* **2012**, *427*, 452−459.
(18) Wooster, T. J.; Golding, M.; Sanguansri, P. Impact of Oil Type on Nanoemulsion Formation and Ostwald Ripening Stability. *Langmuir* **2008**, *24*, 12758−12765.
(19) Puertas, A. M.; Voigtmann, T. Microrheology of Colloidal Systems. *J. Phys.: Condens. Matter* **2014**, *26*, No. 243101.
(20) Scheffold, F.; Romer, S.; Cardinaux, F.; Bissig, H.; Stradner, A.; Rojas-Ochoa, L. F.; Trappe, V.; Urban, C.; Skipetrov, S. E.; Cipelletti, L.; Schurtenberger, P. New Trends in Optical Microrheology of Complex Fluids and Gels. *Prog. Colloid Polym. Sci.* **2004**, *123*, 141−146.
(21) Kumar, N.; Mandal, A. Oil-in-water nanoemulsion stabilized by polymeric surfactant: Characterization and properties evaluation for enhanced oil recovery. *Eur. Polym. J.* **2018**, *109*, 265−276.
(22) MacKintosh, F. C.; Schmidt, C. F. Microrheology. *Curr. Opin. Colloid Interface Sci.* **1999**, *4*, 300−307.
(23) Cicuta, P.; Donald, A. M. Microrheology: A Review of the Method and Applications. *Soft Matter* **2007**, *3*, 1449−1455.
(24) Kheawfu, K.; Pikulkaew, S.; Rades, T.; Müllertz, A.; Okonogi, S. Development and Characterization of Clove Oil Nanoemulsions and Self-Microemulsifying Drug Delivery Systems. *J. Drug Delivery Sci. Technol.* **2018**, *46*, 330−338.
(25) Dammak, I.; de Carvalho, R. A.; Trindade, C. S. F.; Lourenço, R. V.; do Amaral Sobral, P. J. Properties of Active Gelatin Films Incorporated with Rutin-Loaded Nanoemulsions. *Int. J. Biol. Macromol.* **2017**, *98*, 39−49.
(26) Chang, Y.; McClements, D. J. Optimization of Orange Oil Nanoemulsion Formation by Isothermal Low-Energy Methods: Influence of the Oil Phase, Surfactant, and Temperature. *J. Agric. Food Chem.* **2014**, *62*, 2306−2312.
(27) Ghosh, V.; Mukherjee, A.; Chandrasekaran, N. Eugenol-Loaded Antimicrobial Nanoemulsion Preserves Fruit Juice against, Microbial Spoilage. *Colloids Surf., B* **2014**, *114*, 392−397.
(28) Di Lorenzo, F.; Seiffert, S. Macro- and Microrheology of Heterogeneous Microgel Packings. *Macromolecules* **2013**, *46*, 1962−1972.
(29) Shafiq, S.; Shakeel, F.; Talegaonkar, S.; Ahmad, F. J.; Khar, R. K.; Ali, M. Development and Bioavailability Assessment of Ramipril Nanoemulsion Formulation. *Eur. J. Pharm. Biopharm.* **2007**, *66*, 227−243.
(30) Öztürk, M.; Duru, M. E.; Kivrak, Ş.; Mercan-Doğan, N.; Türkoglu, A.; Özler, M. A. *In Vitro* Antioxidant, Anticholinesterase and Antimicrobial Activity Studies on Three Agaricus Species with Fatty Acid Compositions and Iron Contents: A Comparative Study on the Three Most Edible Mushrooms. *Food Chem. Toxicol.* **2011**, *49*, 1353−1360.
(31) Row, C. R.; Sheskey, P. J.; Quinn, M. E. *Handbook of Pharmaceutical Excipients*, 6th ed.; Libros Digitales-Pharmaceutical Press, 2009; Vol. *215*, pp 330−336.
(32) Kothekar, S. C.; Ware, A. M.; Waghmare, J. T.; Momin, S. A. Comparative Analysis of the Properties of Tween-20, Tween-60, Tween-80, Arlacel-60, and Arlacel-80. *J. Dispersion Sci. Technol.* **2007**, *28*, 477−484.
(33) Glenn, K. M.; Moroze, S.; Palepu, R. M.; Bhattacharya, S. C. Effect of Ethylene Glycol on the Thermodynamic and Micellar Properties of Tween 40, 60, and 80. *J. Dispersion Sci. Technol.* **2005**, *26*, 79−86.
(34) Kim, J. H.; Lee, K. H. Effect of PEG Additive on Membrane Formation by Phase Inversion. *J. Membr. Sci.* **1998**, *138*, 153−163.
(35) Chakrabarty, B.; Ghoshal, A. K.; Purkait, M. K. Effect of Molecular Weight of PEG on Membrane Morphology and Transport Properties. *J. Membr. Sci.* **2008**, *309*, 209−221.
(36) Chong, W. T.; Tan, C. P.; Cheah, Y. K.; Lajis, A. F. B.; Dian, N. L. H. M.; Kanagaratnam, S.; Lai, O. M. Optimization of Process Parameters in Preparation of Tocotrienol-Rich Red Palm Oil-Based Nanoemulsion Stabilized by Tween80-Span 80 Using Response Surface Methodology. *PLoS One* **2018**, *13*, 1−22.

https://dx.doi.org/10.1021/acsomega.0c05033
ACS Omega 2021, 6, 559−568

(37) Shah, A. V.; Desai, H. H.; Thool, P.; Dalrymple, D.; Serajuddin, A. T. M. Development of Self-Microemulsifying Drug Delivery System for Oral Delivery of Poorly Water-Soluble Nutraceuticals. *Drug Dev. Ind. Pharm.* **2018**, *44*, 895−901.
(38) Kokkoli, E.; Zukoski, C. F. Effect of Solvents on Interactions between Hydrophobic Self-Assembled Monolayers. *J. Colloid Interface Sci.* **1999**, *209*, 60−65.
(39) Borhade, V.; Pathak, S.; Sharma, S.; Patravale, V. Clotrimazole Nanoemulsion for Malaria Chemotherapy. Part I: Preformulation Studies, Formulation Design and Physicochemical Evaluation. *Int. J. Pharm.* **2012**, *431*, 138−148.
(40) Sessa, M.; Balestrieri, M. L.; Ferrari, G.; Servillo, L.; Castaldo, D.; D'Onofrio, N.; Donsì, F.; Tsao, R. Bioavailability of Encapsulated Resveratrol into Nanoemulsion-Based Delivery Systems. *Food Chem.* **2014**, *106*, 1460−1466.
(41) Gupta, A.; Badruddoza, A. Z. M.; Doyle, P. S. A General Route for Nanoemulsion Synthesis Using Low-Energy Methods at Constant Temperature. *Langmuir* **2017**, *33*, 7118−7123.
(42) Shen, Q.; Wang, Y.; Zhang, Y. Improvement of Colchicine Oral Bioavailability by Incorporating Eugenol in the Nanoemulsion as an Oil Excipient and Enhancer. *Int. J. Nanomed.* **2011**, *6*, 1237−1243.
(43) Seibert, J. B.; Bautista-Silva, J. P.; Amparo, T. R.; Petit, A.; Pervier, P.; dos Santos Almeida, J. C.; Azevedo, M. C.; Silveira, B. M.; Brandão, G. C.; de Souza, G. H. B.; de Medeiros Teixeira, L. F.; dos Santos, O. D. H. Development of Propolis Nanoemulsion with Antioxidant and Antimicrobial Activity for Use as a Potential Natural Preservative. *Food Chem.* **2019**, *287*, 61−67.
(44) Guttoff, M.; Saberi, A. H.; Mcclements, D. J. Formation of Vitamin D Nanoemulsion-Based Delivery Systems by Spontaneous Emulsification: Factors Affecting Particle Size and Stability. *Food Chem.* **2015**, *171*, 117−122.
(45) Ujjwal, R. R.; Sharma, T.; Sangwai, J. S.; Ojha, U. Rheological Investigation of a Random Copolymer of Polyacrylamide and Polyacryloyl Hydrazide (PAM-*ran*-PAH) for Oil Recovery Applications. *J. Appl. Polym. Sci.* **2017**, *134*, 44648.
(46) Tan, Q.; Liu, X.; Fu, X.; Li, Q.; Dou, J.; Zhai, G. Current Development in Nanoformulations of Docetaxel. *Expert Opin. Drug Delivery* **2012**, *9*, 975−990.
(47) Ali, M. S.; Alam, M. S.; Alam, N.; Anwer, T.; Safhi, M. M. A. Accelerated Stability Testing of a Clobetasol Propionate-Loaded Nanoemulsion as per ICH Guidelines. *Sci. Pharm.* **2013**, *81*, 1089−1100.
(48) Borhade, V.; Pathak, S.; Sharma, S.; Patravale, V. Clotrimazole Nanoemulsion for Malaria Chemotherapy. Part II: Stability Assessment, *In Vivo* Pharmacodynamic Evaluations and Toxicological Studies. *Int. J. Pharm.* **2012**, *431*, 149−160.
(49) Kumar, N.; Mandal, A. Thermodynamic and physicochemical properties evaluation for formation and characterization of oil-in-water nanoemulsion. *J. Mol. Liq.* **2018**, *266*, 147−159.
(50) Liang, R.; Xu, S.; Shoemaker, C. F.; Li, Y.; Zhong, F.; Huang, Q. Physical and antimicrobial properties of peppermint oil nanoemulsions. *J. Agric. Food Chem.* **2012**, *60*, 7548−7455.
(51) Pal, N.; Kumar, N.; Mandal, A. Stabilization of dispersed oil droplets in nanoemulsions by synergistic effects of the gemini surfactant, PHPA polymer, and silica nanoparticle. *Langmuir* **2019**, *35*, 2655−2667.

https://dx.doi.org/10.1021/acsomega.0c05033
ACS Omega 2021, 6, 559−568